Cancer Management and Research

Dovepress

open access to scientific and medical research

Open Access Full Text Article

ORIGINAL RESEARCH

MicroRNA-32 and MicroRNA-548a Promote the Drug Sensitivity of Non-Small Cell Lung Cancer Cells to Cisplatin by Targeting ROBO1 and Inhibiting the Activation of Wnt/β-Catenin Axis

This article was published in the following Dove Press journal:
Cancer Management and Research

Jian Zheng[1]
Xiaoxi Li[2]
Cunwei Cai[3]
Chengyu Hong[1]
Bin Zhang[4]

[1]Department of Thoracic Medicine, Cancer Hospital of China Medical University, Liaoning Cancer Hospital & Insititute, Shenyang, Liaoning, 110042, People's Republic of China; [2]Central Laboratory, Cancer Hospital of China Medical University, Liaoning Cancer Hospital & Insititute, Shenyang, Liaoning, 110042, People's Republic of China; [3]Department of Pathology, Cancer Hospital of China Medical University, Liaoning Cancer Hospital & Insititute, Shenyang, Liaoning, 110042, People's Republic of China; [4]Department of Oncology, The First Affiliated Hospital of Dalian Medical University, Dalian, Liaoning, 116011, People's Republic of China

Background: The roles of microRNA (miR)-32 and miR-548a in non-small cell lung cancer (NSCLC) have been studied. But their influences on NSCLC cells to cisplatin (DDP) resistance remain elusive. This study estimated the mechanisms of miR-32 and miR-548a in NSCLC cells to DDP.

Methods: Differentially expressed miRs in DDP-sensitive and resistant tissues were screened out using a GSE56036 chip. Then the predictive efficacies of miR-32 and miR-548a on DDP resistance were analyzed in NSCLC patients. The target mRNAs of miR-548a and miR-32 were predicted. miR-548a and miR-32 were knocked down to assess the influences of miR-32 and miR-548a on NSCLC growth. DDP-resistant cells were constructed and miR-32 and miR-548a expression was detected in resistant cells. After miR-32 and miR-548a knockdown, the IC50 value of DDP was detected. Then, the activation level of Wnt/β-catenin pathway was detected. The roles of miR-32 and miR-548a in NSCLC growth in vivo were detected by tumorigenesis experiment.

Results: miR-32 and miR-548a were poorly expressed in DDP-resistant NSCLC. miR-32 and miR-548a mimic enhanced the DDP sensitivity of NSCLC cells. Both miR-32 and miR-548a targeted ROBO1, and overexpression of ROBO1 inhibited the promotion of miR-32 and miR-548a mimic on DDP sensitivity. ROBO1 activated the Wnt/β-catenin pathway, thus enhancing the DDP resistance.

Conclusion: miR-32 and miR-548a target ROBO1 and inhibit Wnt/β-catenin activation, thus promoting the drug sensitivity of NSCLC cells to DDP.

Keywords: non-small cell lung cancer, miR-32, miR-548a, cisplatin resistance, ROBO1, Wnt/β-catenin pathway

Introduction

Lung cancer (LC) represents a chief cause of cancer-related mortality globally, and about 85% of LC cases show histological subtypes, referred to non-small cell lung cancer (NSCLC).[1] For terminal NSCLC, the cytotoxic chemotherapy, tyrosine kinase inhibitor targeted therapy and checkpoint blockade immunotherapy have been proven to improve the overall survival.[2] Particularly, cisplatin (DDP)-based chemotherapy has been accepted as the first-line approach for NSCLC after resection.[3] Unfortunately, patients with NSCLC initially show a good response to chemotherapy; however, some patients develop DDP resistance in the later process,

Correspondence: Jian Zheng
Department of Thoracic Medicine, Cancer Hospital of China Medical University, Liaoning Cancer Hospital & Insititute, NO. 44 Xiaoheyan Road, Dadong District, Shenyang, Liaoning, 110042, People's Republic of China
Tel/Fax +86-24-31916363
Email zhengjian_2020@163.com

submit your manuscript | www.dovepress.com
DovePress
http://doi.org/10.2147/CMAR.S295003

which greatly limits the effectiveness of chemotherapy.[4] The cellular resistance to DDP is a multifactorial phenomenon, concerning many biological molecules and interrelated pathways.[5] It is reported that chemotherapy resistance is associated with increased drug efflux, target conversion, cell cycle checkpoint changes, apoptosis suppression and enhanced DNA damage repair.[6] At present, further elucidating the molecular mechanism and determining novel biomarkers of NSCLC resistance remain the urgent issues to be solved in oncology to improve the therapeutic effect of NSCLC.

MicroRNAs (miRs) are small noncoding RNA molecules consisting of 18–23 nucleotides, which exert influences on posttranscriptional modulation of gene expression.[7,8] miRs commonly participate in cellular proliferation, apoptosis, differentiation, angiogenesis and metabolic stress, thus serving as tumor suppressors or oncogenes.[8,9] Aberrant miR expression is also implicated in a wide range of pathways contributing to the cellular resistance to DDP in NSCLC.[10–12] In the current study, we screened 116 differentially expressed miRs from a DDP-resistant NSCLC microarray GSE56036 in GEO database, including miR-32 and miR-548a. miR-32 has recently been reported to participate in various critical processes of human malignancies, such as colorectal cancer,[13] gastric cancer[14] and breast cancer.[15] miR-32 expression is notably reduced in NSCLC, and the reduction of miR-32 contributes to tumor stage and lymph node metastasis.[16] Li et al have unveiled that upregulated miR-32 expression represses epithelial mesenchymal transformation and NSCLC cell metastasis.[17] Moreover, accumulating evidence has revealed that miR-548 suppresses cancer cell proliferation and facilitates apoptosis, thus functioning as a tumor suppressor in tumors of lung, breast and pancreatic.[18,19] However, the specific mechanism of miR-32 and miR-548a in DDP resistance in NSCLC patients is unclear. In view of this, we performed in vivo and in vitro experiments to identify the underlying mechanisms of miR-32 and miR-548a in DDP resistance, which shall shed lights on the management of chemoresistance in NSCLC patients.

Materials and Methods

Microarray Analysis

GEO database (https://www.ncbi.nlm.nih.gov/geo/) was adopted to obtain the gene expression chip of LC. Firstly, the datasets of gene expression in drug-resistant LC tissues or cells and DDP-sensitive tumor tissues and cells were processed with R language. Furthermore, the expression profile, pathway enrichment and gene enrichment map were achieved. Then, TargetScan (http://www.targetscan.org/vert_72/) and miRDB (http://mirdb.org/) website predicted the targeted mRNAs of miR-32 and miR-548a. Kaplan-Meier website was adopted to predict the expression of miR-32 and miR-548a and the life cycle of NSCLC patients.

Sample Collection

From March 2017 to January 2019, we recruited DDP-resistant (n = 36) and sensitive (n = 42) NSCLC patients from the Cancer Hospital of China Medical University. Using the proportion of changes in tumor volume after treatment, the patients were grouped into four subgroups: i) Complete response (CR; no tumor); ii) partial response (PR; tumor shrinkage by > 50%); iii) stable disease (tumor shrinkage by < 50% or tumor enlargement by < 25%); and iv) progressive disease (PD; tumor enlargement by > 25%). Patients in the CR and PR groups were defined as DDP-sensitive, and those in the SD and PD groups were defined as DDP-resistant. The experimental scheme was ratified by the Ethics Committee of the Cancer Hospital of China Medical University and followed the Helsinki Declaration (Approval No. CMU2017026). All the subjects involved were fully informed of the objective of the study and signed informed consent before sampling. NSCLC patients receiving DDP and surgery were included and those with a history of serious diseases, such as heart disease and allergies were excluded. The tumor tissues were collected from the included patients through surgery.

RT-qPCR

Total RNA was isolated by RNAiso Plus reagent (Takara, Dalian, China), and then lncRNA, miRs and target genes were reverse transcribed using M-MLV RT Kit (Thermo Fisher Scientific, Waltham, MA, USA) or TaqMan miRNA RT Kit (Thermo Fisher Scientific). In order to detect the RNA level, SYBR Green PCR Master Mix (Thermo Fisher Scientific) were used for qPCR analysis, which was run on 7500 real-time PCR system (Thermo Fisher Scientific). The expression was measured using $2^{-\Delta\Delta CT}$ method with GAPDH or U6 as the parameter. The primer sequences are presented in Table 1.

Establishment of DDP-Resistant Cell Line

A549 and H1299 cells were provided by the cell bank of Chinese Academy of Sciences. DDP-resistant A549/DDP cells were obtained from the typical culture collection

Table 1 Primer Sequences for RT-qPCR

Gene	Primer Sequence (5′-3′)
miR-32	F: TTGCACATTACTAAGTTGC R: GAACATGTCTGCGTATCTC
miR-548a	F: AAACTGGCAATTACTTTTGC R: GAACATGTCTGCGTATCTC
U6	F: CTCGCTTCGGCAGCACAT R: TTTGCGTGTCATCCTTGCG
ROBO1	F: AGTGAGCCTCAGTTCATCCAGC R: GCTCCAATACCTGCTATGAAGGC
Wnt1	F: CTCTTCGGCAAGATCGTCAACC R: CGATGGAACCTTCTGAGCAGGA
CTNNB1	F: CACAAGCAGAGTGCTGAAGGTG R: GATTCCTGAGAGTCCAAAGACAG
GAPDH	F: GTCTCCTCTGACTTCAACAGCG R: ACCACCCTGTTGCTGTAGCCAA

Abbreviations: RT-qPCR, reverse transcription quantitative polymerase chain reaction; miR, microRNA; ROBO1, roundabout guidance receptor 1; CTNNB1, catenin beta 1; GAPDH, glyceraldehyde-3-phosphate dehydrogenase; F, forward; R, reverse.

center of the United States. DDP-resistant H1299 (H1299/DDP) cells were established by exposure to DDP with gradually enhanced concentrations. In short, H1299 cells were added with 0.5 μg/mL DDP (Sigma-Aldrich, Merck KGaA, Darmstadt, Germany). When resistant to the current concentration, cells were added with DDP with increased concentration gradually until 15.2 μg/mL. If the cells survived in 10 μg/mL DDP for 2 months, they were DDP-resistant. Parental cells were incubated in F12K or RPMI-1640 with 10% fetal bovine serum (FBS) (all from Thermo Fisher Scientific). Resistant were cultured in RPMI-1640 supplemented with 10% FBS and 2 μg/mL DDP to keep drug resistant. All cells were cultured in a moist chamber containing 5% CO_2 at 37°C until the logarithmic growth phase.

Cell Counting Kit-8 (CCK-8) Assay

Cells were plated at 2.0×10^3 cells/well in 96-well plates with 10 μM DDP at 0, 0.01, 0.1, 1, 10 and 100 μg/mL, respectively. CCK-8 Kit (Dojindo, Kumamoto, Japan) was used to record the absorbance at 450 nm, the activity curve was drawn and the IC50 was estimated.

Colony Formation Assay

The cells were plated for 2–3 weeks in 6-well plates (500 cells/well), then immobilized at 20°C in 100% methanol, and stained for 20 min with 0.5% crystal violet (Sigma-Aldrich). Next, the colonies larger than 50 μm were calculated by Quantum One software (Bio-Rad, Hercules, CA, USA). Finally, the colonies were observed (×10) and calculated under the light microscope (BX-42, Olympus, Tokyo, Japan).

5-Ethynyl-2′-Deoxyuridine (EdU) Labeling Assay

About 5×10^3 cells were plated in 96-well plates with 100 μL DMEM, and added with 0 μM DDP for 6 h. Then cell growth was testified by Cell-Light EdU Apollo 567 in vitro Kit (Ribobio, Guangzhou, China). Next, cells were cultured for 2 h in the medium containing 50 μL EdU and fixed for 30 min with 4% paraformaldehyde. Following that, cells were added with 1 x reaction mixture (100 μL) for 30 min, and counterstained for 30 min in the dark with 1 x Hoechst 33342. Finally, the fluorescence images were taken using a microscope (BX51, Olympus).

Flow Cytometry

The cells were resuspended to $1–5 \times 10^5$/mL in binding buffer (500 μL), followed by incubation with annexin V-FITC (5 μL) and PI (5 μL) for 30 min in the dark at 20°C. Apoptosis was measured by flow cytometer (FACS Calibur, BD Biosciences, San Jose, CA, USA) within half an hour. Data were processed by Cellquest Pro software 3.3.

Detection of Lactate Dehydrogenase (LDH)

Each well contained 1.5×10^5 A549 and H1299 parental or drug-resistant cells, which were cultured overnight in 24-well plates. The supernatant was collected and added to 96-well black culture plate (200 μL/well). LDH release levels were evaluated using the LDH cytotoxicity test kit (Beyotime, Shanghai, China). Enzyme linked immunosorbent assay (ELISA) was adopted for determination of the absorbance at 450 nm.

Dual-Luciferase Assay

The wild-type ROBO1 (ROBO1-wt) or mutant (ROBO1-mt) sequence containing putative binding sites of miR-32 and miR-548a, respectively, were inserted into the psiCHECK-2 plasmid (Promega, Madison, WI, USA). Then, the reporter genes were transfected into 293T cells together with miR-32 and miR-548a mimic or mimic NC. About 48 h later,

luciferase activity was estimated by the detection system (Promega).

Immunofluorescence

The sterilized slide was placed in 6-well plates with about 3×10^4 cells/well. Following 12-h treatment with DDP, cells were fixed for 30 min in 4% paraformaldehyde, then permeated for 10 min in 0.5% Triton X-100, and sealed for 30 min using 1% albumin bovine V (ServiceBio, Changchun, Jilin, China). The cells were subjected to overnight incubation with primary antibody at 4°C and 1-h incubation with secondary antibody (Antgene, Wuhan, Hubei, China) in the dark. Subsequently, the nuclei were dyed with DAPI (Antgene) under dark conditions. Images were acquired using an automatic microscope (BX63, Olympus).

Tumor Xenograft in Nude Mice

Male BALB/C nude mice (Changsha experimental animal Co., Ltd., Changsha, Hunan, China) got subcutaneous injection of A549-R cells stably overexpressing miR-32 and miR-548a via the armpit of the right-side forelimbs. DDP (5 mg/kg; Solarbio, Beijing, China) was administered intraperitoneally twice a week when mice developed obvious tumors. The tumor size was measured six times every three days. Twenty-five days after injection, all animals were killed and the tumors were removed for immunohistochemistry. Tumor volume was estimated: V = a *b^2 * 0.52 (mm^3), in which "a" indicates the longest diameter and "b" indicates the shortest diameter. The animal experimental protocol was approved by the Committee on the Ethics of Animal Experiments of the Cancer Hospital of China Medical University (Approval No. CMU2018001605). All animal procedures were performed in line with the Guide for the Care and Use of Laboratory animals published by the National Institutes of Health, Bethesda, Maryland, USA.

Immunohistochemistry

After fixing in 4% paraformaldehyde and embedding in paraffin, the tumor tissue sections were deparaffined, hydrated, and antigen was repaired using 10 mM sodium citrate (pH 6.0). After removal of endogenous peroxidase with 3% H_2O_2, the sample was sealed for 30 min with albumin (ServiceBio) and then incubated overnight with primary antibody at 4°C. The reaction was visualized with 3,3′-diaminobenzidine kit (ServiceBio) and stained with hematoxylin for 1 min. The image was gained using the microscope.

Terminal Deoxynucleotidyl Transferase (TdT)-Mediated dUTP Nick End Labeling (TUNEL)

After routine dewaxing and rehydration, the tumor tissue sections were tested as per the kit (Roche, Indianapolis, IN, USA). Shortly, the slices were incubated for 45 min at 37°C in terminal glucosyltransferase reaction cocktail, and treated with Click-iT reaction cocktail. The nuclei were stained with hematoxylin.

Statistical Analysis

All tests were made in triplicate. Data analysis was done using the SPSS 20.0 (IBM Corp., Armonk, NY, USA) and GraphPad Prism 6.0 (GraphPad Software Inc., San Diego, CA, USA). All data were described as mean ± standard deviation (SD). The homogeneity of variance was tested by Levene test. Data after Levene test were analyzed by one-way analysis of variance (ANOVA) and Tukey's test. $P < 0.05$ represented statistical significance at the 5% level, $p < 0.01$ at the 1% level, and $p < 0.001$ at the 0.1% level.

Results

miR-32 and miR-548a are Poorly Expressed in DDP-Resistant NSCLC Cells

GSE56036, a DDP-resistant NSCLC chip including data of 34 DDP-sensitive NSCLC tissues and 24 resistant tissues, was downloaded from GEO database. By setting log FC > 1 and Adj p value < 0.05 as the screening thresholds, 116 differentially expressed miRs (Figure 1A) were screened. Among them, miR-32 and miR-548a were significantly lowered in DDP-resistant NSCLC tissues. Subsequently, 36 cases of DDP-resistant tumor tissues and 42 cases of DDP-sensitive tumor tissues were analyzed. RT-qPCR showed that miR-32 and miR-548a expression in DDP-resistant tumor tissues was notably decreased (Figure 1B). Furthermore, a receiver operating characteristic (ROC) curve was adopted to estimate the predictive effects of miR-32 and miR-548a on DDP resistance of NSCLC patients. It was found that both miR-32 and miR-548a had good predictive effects on DDP resistance of NSCLC patients (Figure 1C). Subsequently, we predicted the expression of miR-32 and miR-548a and the life cycle of NSCLC patients through Kaplan-Meier website. Patients with high expression of miR-32 or miR-548a

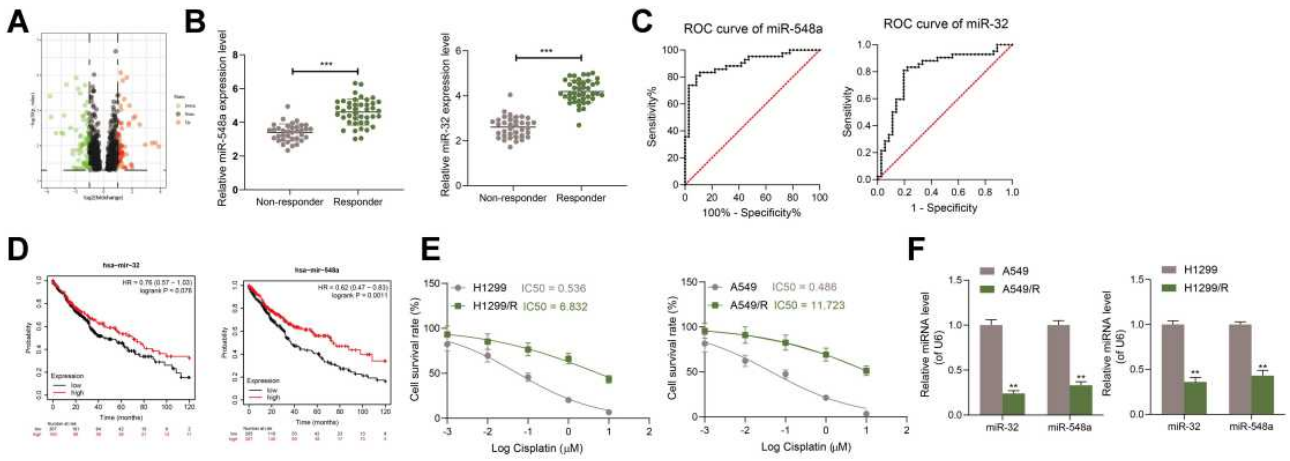

Figure 1 miR-32 and miR-548a are poorly expressed in DDP-resistant NSCLC cells. (**A**) Differentially expressed miRs in GSE56036 chip; (**B**) expression of miR-32 and miR-548a in tumor tissues of 36 patients with DDP-resistant NSCLC and 42 patients with DDP-sensitive NSCLC measured by RT-qPCR; (**C**) the predictive efficacies of miR-32 and miR-548a on DDP resistance in NSCLC patients testified by an ROC curve; (**D**) Kaplan Meier website predicted the expression of miR-32 and miR-548a and the life cycle of NSCLC patients; (**E**) IC50 values verified by CCK-8; (**F**) expression of miR-32 and miR-548a in parental or resistant A549 and H1299 cells examined by RT-qPCR. In Figures (**E** and **F**) each experiment was conducted three times; the data were described as mean ± SD and processed by two-way ANOVA and Tukey's test, $^{**}p < 0.01$, $^{***}p < 0.001$.

had higher survival rate in TCGA-LUAD database (Figure 1D). To estimate the effects of miR-32 and miR-548a on DDP resistance, A549-R and H1299-R cells were constructed by exposing cells to DDP at gradient concentrations. CCK-8 test elicited that IC50 values of DDP were evidently increased (Figure 1E), indicating that the drug-resistant cell line was successfully constructed. Then, the expression of miR-32 and miR-548a in parental and resistant cells was measured. It was found that the expression of miR-32 and miR-548a was obviously decreased in A549-R and H1299-R cells (Figure 1F). Briefly, the abnormal low expression of miR-32 and miR-548a is strongly related to drug resistance of NSCLC cells.

Overexpression of miR-32 and miR-548a Enhances Drug Sensitivity of NSCLC Cells to DDP

To confirm the effects of miR-32 and miR-548a on DDP resistance, we transfected miR-32 and miR-548a mimic into A549-R and H1299-R cells, and confirmed the successful transfection by RT-qPCR (Figure 2A). Subsequently, A549-R and H1299-R cells transfected with miR-32 and miR-548a mimic were exposed to DDP at gradient concentrations. CCK-8 method unveiled that miR-32 and miR-548a mimic transfection significantly elevated DDP sensitivity (Figure 2B). Furthermore, A549-R and H1299-R cells overexpressing miR-32 and miR-548a were exposed to 10 μM DDP for 12 h. The number of clone formation and EdU-positive cells were clearly reduced (Figure 2C–D). Flow cytometry also showed that overexpressing miR-32 and miR-548a enhanced the percentage of apoptosis (Figure 2E) and increased the release of LDH in DDP-treated cells (Figure 2F).

miR-32 and miR-548a Target ROBO1

To clarify the downstream mechanisms of miR-32 and miR-548a, we downloaded the DDP-resistant gene expression chip GSE21656 from GEO database, and screened 242 differentially expressed mRNAs, of which 69 were upregulated and 173 were downregulated (Figure 3A–B). Subsequently, Starbase predicted the common targeted mRNAs of miR-32 and miR-548a, and the outcomes were further intersected with the upregulated genes in GSE21656 chip, and ROBO1 was obtained (Figure 3C). Robo1 expression in tumor tissues of 36 patients with DDP-resistant and 42 patients with DDP-sensitive NSCLC was further detected. ROBO1 in tumor tissues of patients with drug resistance was clearly increased (Figure 3D). Furthermore, ROBO1 was increased in the A549-R and H1299-R cells but decreased after further transfection of miR-32 and miR-548a mimic (Figure 3E). Therefore, we designed a dual-luciferase experiment to verify the targeted relation between miR-32 and miR-548a and 3′UTR sequence of ROBO1. The luciferase activity was evidently decreased upon transfection of miR-32 and miR-548a mimic and ROBO1-wt, while that

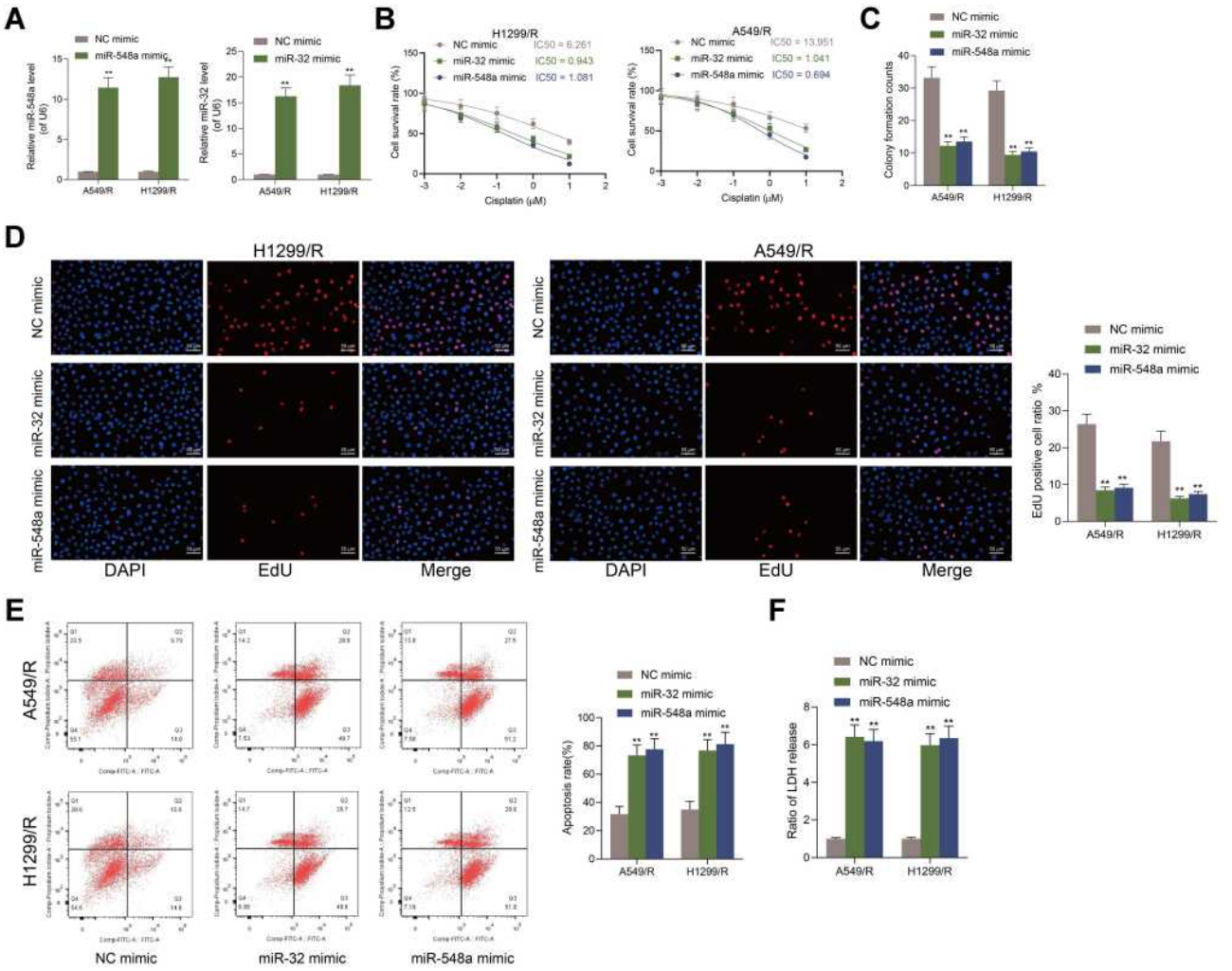

Figure 2 Overexpression of miR-32 and miR-548a enhances drug sensitivity of NSCLC cells to DDP. (**A**) RT-qPCR detected miR-32 and miR-548a expression in A549-R/H1299-R cells; (**B**) CCK-8 kit detected the IC50 value; (**C**) A549-R/H1299-R cells overexpressing miR-32 and miR-548a were exposed to 10 μM DDP for 12 h, and then cells were used for colony formation assay; (**D**) the number and proportion of EdU-positive cells examined by EdU staining; (**E**) apoptosis rate identified by flow cytometry; (**F**) The LDH content detected by a LDH kit. Each experiment was conducted three times, and the data were described as mean ± SD and processed by two-way ANOVA and Tukey's test, $^{**}p < 0.01$.

in the cells upon transfection of mimic NC or ROBO1-mt had no significant change (Figure 3F–G). Briefly, miR-32 and miR-548a target ROBO1.

Overexpression of ROBO1 Blocks the Effects of miR-32 and miR-548a Mimic on DDP Sensitivity

To verify ROBO1 role in DDP resistance, overexpression plasmid of ROBO1 was further transfected into A549-R and H1299-R cells stably overexpressing miR-32 and miR-548a. The transfection was verified by RT-qPCR (Figure 4A). The IC50 values to DDP were evidently increased (Figure 4B). EdU-positive cells were multiplied after DDP treatment (Figure 4C), apoptotic cells were decreased (Figure 4D), the content of LDH was significantly decreased (Figure 4E).

ROBO1 Promotes DDP Resistance by Activating Wnt/β-Catenin Axis

Robo1 stimulates the occurrence of colorectal cancer by activating Wnt/β-catenin axis.[20] Therefore, we first detected the activity of Wnt/β-catenin axis in parental and resistant cells. The levels of CCND1, Wnt1, and β-catenin were remarkably increased, but reduced after further increasing miR-32 and miR-548a expression. The Wnt/β-catenin activation was clearly increased after overexpression of ROBO1 (Figure 5A and B). Immunofluorescence assay showed that the percentage of

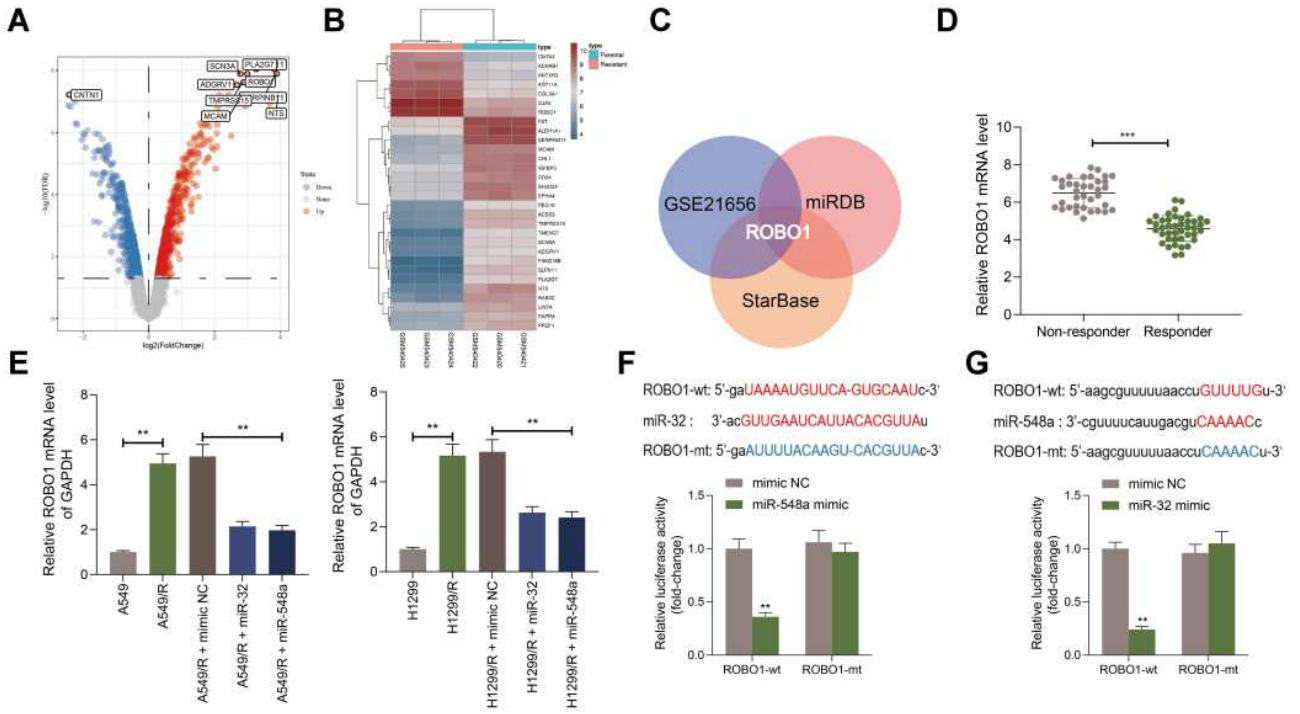

Figure 3 miR-32 and miR-548a target ROBO1. (**A**–**B**) Differentially expressed genes in GSE21656 chip; (**C**) targeted mRNAs of miR-32 and miR-548a predicted on StarBase and miRDB bioinformatic systems, and the results were cross screened with the upregulated genes in GSE21656 chip; (**D**) ROBO1 expression in DDP-resistant and sensitive tissues examined by RT-qPCR; (**E**) RT-qPCR detected ROBO1 in parental and drug-resistant cells; (**F**–**G**) dual-luciferase assay verified the targeting relationships between miR-32/miR-548a and ROBO1. In Figures (**E** and **G**) each experiment was performed three times; the data were described as mean ± SD and processed by two-way ANOVA and Tukey's test, $^{**}p < 0.01$, $^{***}p < 0.001$.

β-catenin into the nucleus of drug-resistant cells was increased, but miR-32 and miR-548a mimic restricted β-catenin nucleation, while OE-ROBO1 averted the restriction of miR-32 and miR-548a on β-catenin nucleation (Figure 5C). LEF/TCF luciferase assay was adopted to detect the activation level of Wnt/β-catenin. The activity of LEF/TCF luciferase in drug-resistant cells was elevated relative to that in parental cells, but miR-32 and miR-548a inhibited the Wnt/β-catenin activation, while the overexpression of ROBO1 increased the luciferase activity of Wnt/β-catenin (Figure 5D).

Overexpression of miR-32 and miR-548a Inhibits DDP Resistance of NSCLC Cells in vivo

To clarify the effects of miR-32 and miR-548a on DDP resistance in vivo, A549-R cells stably overexpressing miR-32 and miR-548a were subcutaneously injected into nude mice, and DDP was administered to mice on the 15th, 20th and 23rd day, respectively. After measuring the volume of xenograft tumor in mice, we found that miR-32 and miR-548a mimic inhibited the growth of A549-R cells in vivo and promoted the killing effect of DDP on A549 cells (Figure 6A–B). Immunohistochemistry evaluated the levels of Ki67, CTNNB1 and ROBO1 in xenograft tumors, and elicited that miR-32 and miR-548a overexpression inhibited the staining intensity of Ki67, CTNNB1 and ROBO1 (Figure 6C–E). Moreover, TUNEL showed that miR-32 and miR-548a mimic augmented the anticancer effect of DDP on A549-R cells in vivo (Figure 6F).

Discussion

DDP is an antineoplastic, representing the backbone of treatment regimens of myriad malignancies, including NSCLC.[21,22] However, DDP treatment often leads to chemotherapy resistance, eventually resulting in therapeutic failure.[23] Alternation of miR expression caused by chemotherapy drugs in tumor cells has indicated that the mechanism of chemotherapy drug action is concerned with miRs.[24] We demonstrated that miR-32 and miR-548a promoted the DDP sensitivity of NSCLC cells via ROBO1/Wnt/β-catenin axis.

Microarray GSE56036 showed that miR-32 and miR-548a were downregulated in DDP-resistant NSCLC

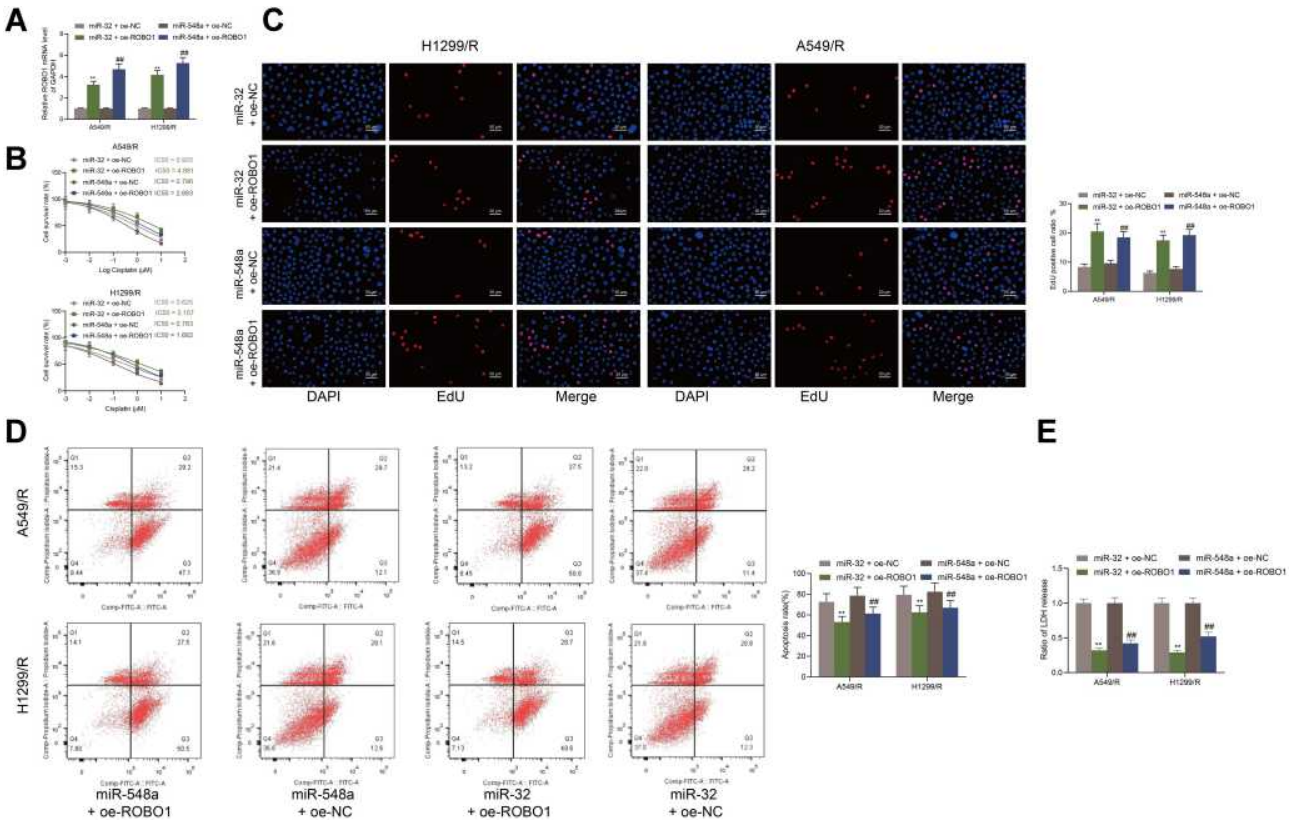

Figure 4 Overexpression of ROBO1 blocks the effects of miR-32 and miR-548a mimic on DDP sensitivity. (**A**) RT-qPCR detected ROBO1 expression in A549-R/H1299-R cells; (**B**) CCK-8 kit detected the IC50 value; (**C**) A549-R/H1299-R cells overexpressing ROBO1 were exposed to 10 μM DDP for 12 h, and the number and proportion of EdU-positive cells examined by EdU staining; (**D**) the apoptosis rate identified by flow cytometry; (**E**) the LDH content detected by a LDH kit. Each experiment was done three times, and the data were exhibited as mean ± SD and processed by two-way ANOVA and Tukey's test; $^{**}p < 0.01$ vs miR-32 + oe- NC; $^{\#\#}p < 0.01$ vs miR-548a + oe-NC.

tissues. ROC curve exhibited that miR-32 and miR-548a had good predictive effects on DDP resistance of NSCLC patients. miR-32 is declined in 5-Fu-induced multidrug-resistant gastric cancer cells, which may represent a molecular target for multidrug resistance elimination.[25] miR-548e-5p is evidently lowered in LC specimens.[26] Additionally, TCGA-LUAD database showed that patients with higher expression of miR-32 and miR-548a had higher survival rate. We successfully constructed DDP-resistant cell lines. miR-32 and miR-548a were notably lowered in resistant cells. Taken together, the abnormal low level of miR-32 or miR-548a linked with drug resistance of NSCLC cells. Then, miR-32 and miR-548a mimic were delivered to A549 and H1299 cells, followed by treatment with DDP of gradient concentrations. The results elicited that overexpression of miR-32 and miR-548a elevated DDP sensitivity of NSCLC cells. miR-32 expression is associated with the efficacy and survival rate of platinum chemotherapy, suggesting the potential of miR-32 in predicting the efficacy and prognosis of NSCLC patients receiving chemotherapy.[24] miR-548-3p, a member of the miR-548 family, may act as an anti-tumor target of LC.[27] miR-548e-5p overexpression can significantly block LC cell proliferation, migration, and invasion.[26] Still, relatively little was known about the effect of miR-548a on drug resistance yet, and our study filled this gap to some degree. We were the first to reveal that miR-32 and miR-548a mimic promoted the DDP sensitivity.

To clarify downstream molecular mechanism of miR-32 and miR-548a, we screened 242 differentially expressed mRNAs from DDP-resistant gene expression microarray GSE21656. Subsequently, Starbase predicted the targeted mRNAs of miR-32 and miR-548a, and cross-screened with the upregulated genes in GSE21656. Finally, ROBO1 was obtained. ROBO1 is an evolutionarily conserved protein, participating in the regulation of axon guidance, axon branching and neuronal cell migration during the central nervous system development.[28] ROBO1 in NSCLC metastasis is negatively correlated with the prognosis, acting as a cancer-promoting oncogene.[29] We exhibited that ROBO1 expression was notably promoted in tumor tissues of drug-resistant patients and in A549 and H1299 cells, while the

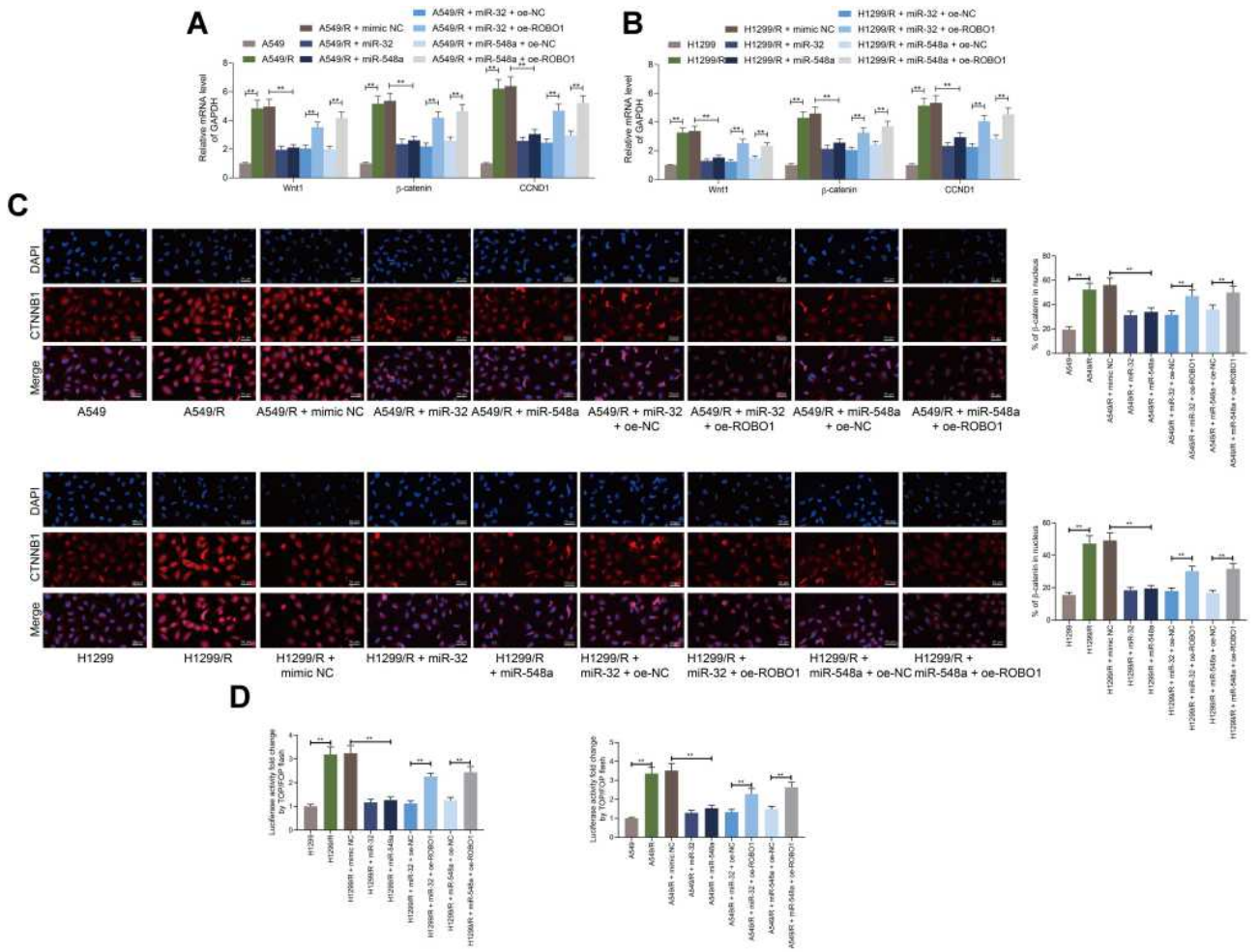

Figure 5 ROBO1 promotes DDP resistance by activating the Wnt/β-catenin axis. (**A**–**B**) RT-qPCR examined expression of Wnt1, β-catenin and CCND1; (**C**) nuclear translocation of β-catenin in cells detected by immunofluorescence; (**D**) the percentage of TCF/LEF luciferase activity was shown as the percentage of relative light units of fire luciferase to Renilla luciferase. Each experiment was done three times, and the data were exhibited as mean ± SD and processed by two-way ANOVA and Tukey's test; $^{**}p < 0.01$.

ROBO1 expression was reduced after further transfection of miR-32 and miR-548a mimic. Dual-luciferase assay identified the target relationships between miR-32 or miR-548a and ROBO1. Briefly, miR-32 and miR-548a targeted ROBO1. To elucidate the influence of ROBO1 on DDP resistance, the overexpression vector of ROBO1 was transfected into A549 and H1299 cells stably overexpressing miR-32 and miR-548a. Our results supported that overexpression of ROBO1 attenuated the effect of miR-32 and miR-548a mimic on DDP sensitivity of NSCLC cells. Suppression of ROBO1 contributes to inhibiting LC cell migration and invasion.[30] Anti-ROBO1 monoclonal antibody possesses antineoplastic activity against NSCLC xenografts.[31] Intriguingly, ROBO1 is also demonstrated to be concerned with paclitaxel sensitivity[32] and chemoresistance in glioblastoma.[33] In sum, miR-32 and miR-548a mimic promoted DDP sensitivity by targeting ROBO1.

Thereafter, we shift to investigating the downstream pathway of ROBO1. ROBO1 can facilitate intestinal tumorigenesis via the activation of Wnt/β-catenin.[34] Canonical Wnt signaling mediated by β-catenin is accepted as a crucial regulator of chemoresistance, and repression of Wnt/β-catenin signaling enhances the sensitivity to chemotherapeutic agents in prostate cancer, pancreatic cancer and urothelial carcinoma of bladder.[35–37] Our results indicated that the levels of Wnt1, β-catenin and CCND1 were remarkably increased in A549-R and H1299-R cells, but decreased after miR-32 and miR-548a upregulation; the activation of Wnt/β-catenin was clearly augmented after overexpression of ROBO1. Wnt activation is common in lung malignancies and contributes to tumor recurrence.[38] As a cooperative target of Wnt, ROBO1 displays reduced expression in Wnt1/DNIIR tumors.[20] Collectively, ROBO1

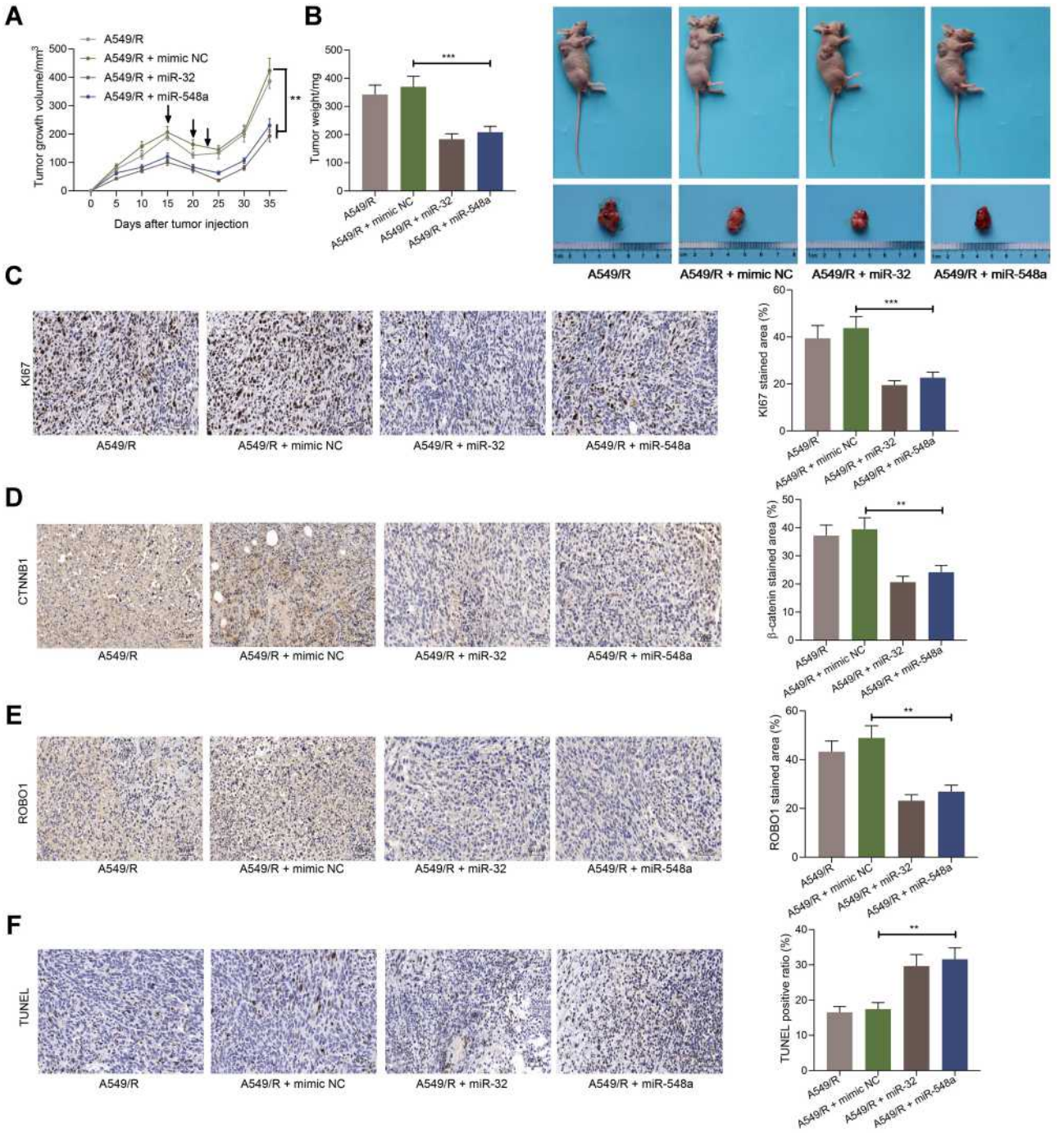

Figure 6 Overexpression of miR-32 and miR-548a inhibits DDP resistance in vivo. (**A**) The growth curve of xenograft tumor formed by A549-R cells (the arrows indicate the time points for DDP administration in mice after cell injection); (**B**) photos of mice and tumors and weight of the xenograft tumors; (**C**–**E**) the staining intensity of Ki67, CTNNB1 and ROBO1 in xenograft tumor was detected by immunohistochemistry; (**F**) the proportion of apoptotic cells in xenograft tumor detected by TUNEL. N = 5 in each group. The data were exhibited as mean ± SD and processed by two-way ANOVA and Tukey's test; $^{**}p < 0.01$, $^{***}p < 0.001$.

upregulation activated the Wnt/β-catenin axis, thus elevating DDP resistance.

Moreover, to clarify the functions of miR-32 and miR-548a on DDP resistance in vivo, we injected A549-R cells stably overexpressing miR-32 and miR-548a into nude mice, and then mice were administered with DDP. miR-32 and miR-548a mimic blocked the growth of A549-R cells in vivo, promoted the killing effect of DDP on A549 cells, and enhanced the antitumor effect of DDP on A549-R cells. Briefly, overexpression of miR-32 and miR-548a suppressed DDP resistance in vivo.

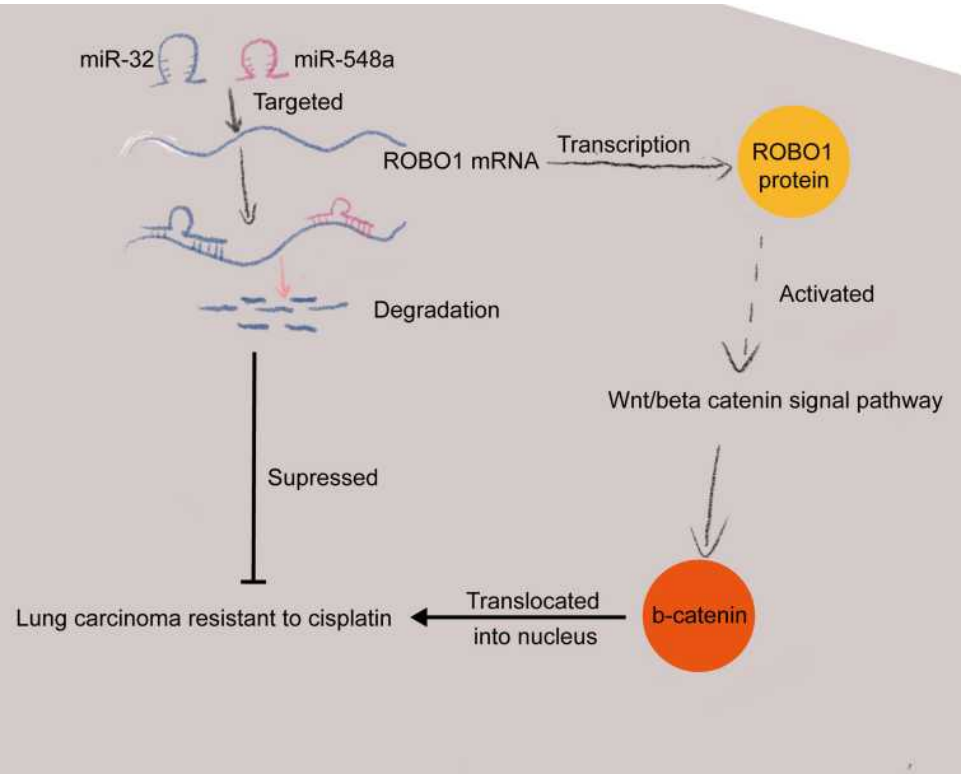

Figure 7 A diagram for the molecular mechanism. miR-32 and miR-548a negatively regulate ROBO1 in NSCLC cells and inhibit Wnt/β-catenin activation, thus promoting the sensitivity of NSCLC cells to DDP.

To sum up, miR-32 and miR-548a stimulated the DDP sensitivity by targeting ROBO1 and inactivating Wnt/β-catenin pathway in NSCLC cells (Figure 7). The study might hint the possibility of miR-32 and miR-548a as potential targets for NSCLC patients with DDP resistance.

Acknowledgments

We thank Hanyu Biomed Center for the help in bioinformatic analysis.

Disclosure

The authors declare no conflicts of interest in this work.

References

1. Herbst RS, Morgensztern D, Boshoff C. The biology and management of non-small cell lung cancer. *Nature*. 2018;553(7689):446–454. doi:10.1038/nature25183
2. Zheng H, Zeltsman M, Zauderer MG, Eguchi T, Vaghjiani RG, Adusumilli PS. Chemotherapy-induced immunomodulation in non-small-cell lung cancer: a rationale for combination chemoimmunotherapy. *Immunotherapy*. 2017;9(11):913–927. doi:10.2217/imt-2017-0052
3. Wei Y, Wu S, Xu W, et al. Depleted aldehyde dehydrogenase 1A1 (ALDH1A1) reverses cisplatin resistance of human lung adenocarcinoma cell A549/DDP. *Thorac Cancer*. 2017;8(1):26–32. doi:10.1111/1759-7714.12400
4. Wang L, Ma L, Xu F, et al. Role of long non-coding RNA in drug resistance in non-small cell lung cancer. *Thorac Cancer*. 2018;9(7):761–768. doi:10.1111/1759-7714.12652
5. Griguer CE, Oliva CR. Bioenergetics pathways and therapeutic resistance in gliomas: emerging role of mitochondria. *Curr Pharm Des*. 2011;17(23):2421–2427. doi:10.2174/138161211797249251
6. Vasan N, Baselga J, Hyman DM. A view on drug resistance in cancer. *Nature*. 2019;575(7782):299–309. doi:10.1038/s41586-019-1730-1
7. Shioya M, Obayashi S, Tabunoki H, et al. Aberrant microRNA expression in the brains of neurodegenerative diseases: miR-29a decreased in Alzheimer disease brains targets neurone navigator 3. *Neuropathol Appl Neurobiol*. 2010;36(4):320–330. doi:10.1111/j.1365-2990.2010.01076.x
8. Zhang B, Pan X, Cobb GP, Anderson TA. microRNAs as oncogenes and tumor suppressors. *Dev Biol*. 2007;302(1):1–12. doi:10.1016/j.ydbio.2006.08.028
9. Wei L, Wang X, Lv L, et al. The emerging role of microRNAs and long noncoding RNAs in drug resistance of hepatocellular carcinoma. *Mol Cancer*. 2019;18(1):147. doi:10.1186/s12943-019-1086-z
10. Drayton RM. The role of microRNA in the response to cisplatin treatment. *Biochem Soc Trans*. 2012;40(4):821–825. doi:10.1042/BST20120055
11. Ma Y, Yuwen D, Chen J, et al. Exosomal transfer of cisplatin-induced miR-425-3p confers cisplatin resistance in NSCLC through activating autophagy. *Int J Nanomedicine*. 2019;14:8121–8132. doi:10.2147/IJN.S221383
12. Wang C, Wang S, Ma F, Zhang W. miRNA328 overexpression confers cisplatin resistance in nonsmall cell lung cancer via targeting of PTEN. *Mol Med Rep*. 2018;18(5):4563–4570. doi:10.3892/mmr.2018.9478
13. Chen E, Li Q, Wang H, et al. MiR-32 promotes tumorigenesis of colorectal cancer by targeting BMP5. *Biomed Pharmacother*. 2018;106:1046–1051. doi:10.1016/j.biopha.2018.07.050

14. Zhao L, Han T, Li Y, et al. The lncRNA SNHG5/miR-32 axis regulates gastric cancer cell proliferation and migration by targeting KLF4. *FASEB J*. 2017;31(3):893–903. doi:10.1096/fj.201600994R
15. Xia H, Long J, Zhang R, Yang X, Ma Z. MiR-32 contributed to cell proliferation of human breast cancer cells by suppressing of PHLPP2 expression. *Biomed Pharmacother*. 2015;75:105–110. doi:10.1016/j.biopha.2015.07.037
16. Bai Y, Wang YL, Yao WJ, et al. Expression of miR-32 in human non-small cell lung cancer and its correlation with tumor progression and patient survival. *Int J Clin Exp Pathol*. 2015;8(1):824–829.
17. Li L, Wu D. miR-32 inhibits proliferation, epithelial-mesenchymal transition, and metastasis by targeting TWIST1 in non-small-cell lung cancer cells. *Onco Targets Ther*. 2016;9:1489–1498. doi:10.2147/OTT.S99931
18. Shi Y, Qiu M, Wu Y, Hai L. MiR-548-3p functions as an anti-oncogenic regulator in breast cancer. *Biomed Pharmacother*. 2015;75:111–116. doi:10.1016/j.biopha.2015.07.027
19. Zhu S, He C, Deng S, et al. MiR-548an, transcriptionally downregulated by HIF1alpha/HDAC1, suppresses tumorigenesis of pancreatic cancer by targeting vimentin expression. *Mol Cancer Ther*. 2016;15(9):2209–2219. doi:10.1158/1535-7163.MCT-15-0877
20. Labbe E, Lock L, Letamendia A, et al. Transcriptional cooperation between the transforming growth factor-beta and Wnt pathways in mammary and intestinal tumorigenesis. *Cancer Res*. 2007;67(1):75–84. doi:10.1158/0008-5472.CAN-06-2559
21. He L, Luo L, Zhu H, et al. FEN1 promotes tumor progression and confers cisplatin resistance in non-small-cell lung cancer. *Mol Oncol*. 2017;11(6):640–654. doi:10.1002/1878-0261.12058
22. Teng JP, Yang ZY, Zhu YM, Ni D, Zhu ZJ, Li XQ. Gemcitabine and cisplatin for treatment of lung cancer in vitro and vivo. *Eur Rev Med Pharmacol Sci*. 2018;22(12):3819–3825. doi:10.26355/eurrev_201806_15266
23. Galluzzi L, Senovilla L, Vitale I, et al. Molecular mechanisms of cisplatin resistance. *Oncogene*. 2012;31(15):1869–1883. doi:10.1038/onc.2011.384
24. Xu S, Li J, Chen L, et al. Plasma miR-32 levels in non-small cell lung cancer patients receiving platinum-based chemotherapy can predict the effectiveness and prognosis of chemotherapy. *Medicine (Baltimore)*. 2019;98(42):e17335. doi:10.1097/MD.0000000000017335
25. Wang Y, Gu X, Li Z, Xiang J, Jiang J, Chen Z. microRNA expression profiling in multidrug resistance of the 5Fuinduced SGC7901 human gastric cancer cell line. *Mol Med Rep*. 2013;7(5):1506–1510. doi:10.3892/mmr.2013.1384
26. Jin D, Guo J, Wu Y, et al. Retraction of "UBE2C, directly targeted by miR-548e-5p, increases the cellular growth and invasive abilities of cancer cells interacting with the EMT marker protein zinc finger E-box binding homeobox 1/2 in NSCLC. *Theranostics*. 2020;10(21):9619. doi:10.7150/thno.50254
27. Wang Z, Wu X, Hou X, et al. miR-548b-3p functions as a tumor suppressor in lung cancer. *Lasers Med Sci*. 2020;35(4):833–839. doi:10.1007/s10103-019-02865-7
28. Sun X, Song S, Liang X, et al. ROBO1 polymorphisms, callosal connectivity, and reading skills. *Hum Brain Mapp*. 2017;38(5):2616–2626. doi:10.1002/hbm.23546
29. Li XX, Jin L, Sun ZF, Gu F, Li WL, Ma YJ. [Robo1 expression in non-small cell lung cancer and its brain metastasis]. *Zhonghua Zhong Liu Za Zhi*. 2013;35(3):198–201. Chinese. doi:10.3760/cma.j.issn.0253-3766.2013.03.008
30. Chen P, Zhao Y, Li Y. [MiR-218 inhibits migration and invasion of lung cancer cell by regulating robo1 expression]. *Zhongguo Fei Ai Za Zhi*. 2017;20(7):452–458. Chinese. doi:10.3779/j.issn.1009-3419.2017.07.03
31. Fujiwara K, Koyama K, Suga K, et al. 90Y-labeled anti-ROBO1 monoclonal antibody exhibits antitumor activity against small cell lung cancer xenografts. *PLoS One*. 2015;10(5):e0125468. doi:10.1371/journal.pone.0125468
32. Eng L, Ibrahim-zada I, Jarjanazi H, et al. Bioinformatic analyses identifies novel protein-coding pharmacogenomic markers associated with paclitaxel sensitivity in NCI60 cancer cell lines. *BMC Med Genomics*. 2011;4:18. doi:10.1186/1755-8794-4-18
33. Siebzehnrubl FA, Silver DJ, Tugertimur B, et al. The ZEB1 pathway links glioblastoma initiation, invasion and chemoresistance. *EMBO Mol Med*. 2013;5(8):1196–1212. doi:10.1002/emmm.201302827
34. Zhang QQ, Zhou DL, Lei Y, et al. Slit2/Robo1 signaling promotes intestinal tumorigenesis through Src-mediated activation of the Wnt/beta-catenin pathway. *Oncotarget*. 2015;6(5):3123–3135. doi:10.18632/oncotarget.3060
35. Garg M, Maurya N. WNT/beta-catenin signaling in urothelial carcinoma of bladder. *World J Nephrol*. 2019;8(5):83–94. doi:10.5527/wjn.v8.i5.83
36. Ram Makena M, Gatla H, Verlekar D, Sukhavasi S, Pandey M, Pramanik K. Wnt/beta-catenin signaling: the culprit in pancreatic carcinogenesis and therapeutic resistance. *Int J Mol Sci*. 2019;20:17. doi:10.3390/ijms20174242
37. Yeh Y, Guo Q, Connelly Z, et al. Wnt/Beta-catenin signaling and prostate cancer therapy resistance. *Adv Exp Med Biol*. 2019;1210:351–378.
38. Krishnamurthy N, Kurzrock R. Targeting the Wnt/beta-catenin pathway in cancer: update on effectors and inhibitors. *Cancer Treat Rev*. 2018;62:50–60. doi:10.1016/j.ctrv.2017.11.002